Photocatalytic degradation of *p*-amino-azo-benzene and *p*-hydroxy-azo-benzene using various heat treated TiO$_2$ as the photocatalyst

L. Gomathi Devi*, G.M. Krishnaiah

Department of Post Graduate Studies in Chemistry, Central College, Bangalore University, Bangalore 560001, India

Abstract

The photocatalytic degradation of azo dyes in aqueous suspensions of TiO$_2$ is comparatively a good method for the removal of these impurities. The extent of degradation is followed by UV–visible and IR spectroscopy. The degradation process is performed with various heat treated TiO$_2$, in which anatase form of TiO$_2$ exhibited marked photocatalytic activity. © 1999 Elsevier Science S.A. All rights reserved.

Keywords: Semiconductor; Infrared spectroscopy; Catalytic properties; Semiconductivity

1. Introduction

The use of azo dyes in textile industries is very well known [1]. These dyes are found to be environmental hazards if they are released into aqueous environment. Popular treatment methods for eliminating dyes from the waste water stream suffers from one or another drawback. Photocatalytic degradation is found to be a very efficient process for mineralisation of organic pollutants in which catalysts are semiconductor particles. Under band gap excitation the semiconductor particles act as short circuited microelectrodes and initiate the oxidation and reduction processes of the adsorbed substrates. In this communication the degradation of *p*-amino azo benzene (PAAB) and *p*-hydroxy azo benzene (PHAB) using the photocatalyst TiO$_2$ is studied [2]. These dyes were chosen for the study, since both have the relative simple structure compared to the complicated structures of the other azo dyes. The effect of TiO$_2$ annealed at different temperatures on the degradation process is also studied. The extent of degradation of the organic dye compound is determined by UV–visible and IR spectroscopic techniques.

2. Experimental procedure

Fine grained powders of rutile and anatase form of TiO$_2$ is prepared by the precipitation method [3]. Diluted titanium tetrachloride solution is mixed with 1 ml of concentrated sulphuric acid followed by approximately 50 ml of ammonia solution to raise the pH to 8.0 with constant stirring. The precipitate is washed with hot water and made free from chloride ions. This precipitate is kept in an oven at 105–120°C for 48 h to remove the water content. This TiO$_2$ was annealed at 600°C for 4–5 h to get the anatase form of TiO$_2$. Further rise in temperature leads to rutile form of TiO$_2$. These structures were confirmed by X-ray diffraction studies (Phillips PW 1050/70/76). No special care was taken to control the particle size during the processes of preparation.

Photodegradation experiments were carried out in quartz cell using a medium pressure 350 W mercury vapour lamp source by direct exposure into the reaction mixture. The wavelength of which peaks around 350–400 nm. Filters were used whenever it was necessary. The photon flux was found to be 7.75 mW/cm^2 as determined by ferrioxalate actinometry [4–6]. 0.165 mM dye solution along with 0.1 wt% of TiO$_2$ was taken for the experiment. The total volume of the solution handled was 200 ml and pH was adjusted whenever it was necessary using standard buffering agents and this was maintained at 25°C using a thermostat. Photocatalytic degradation of azo benzene compounds performed under the deaerated condition shows that, even after 48 h the concentration of the azo compound almost remains constant. This shows that oxygen is necessary for degradation process. Samples for analysis were withdrawn at any desired time interval during irradiation and centrifuged. The extent of decomposition of the organic azo dye compound was determined by UV–visible (Hitachi model 150–200

*Corresponding author.

double beam spectrophotometer) and IR (Nicolet IMPACT 400D FTIR SPECTROMETER) spectroscopy.

3. Results and discussion

Table 1 gives the details of material characteristics for various TiO2 samples. The TiO2 prepared by the precipitation method is further subjected to thermal treatment.

The TiO2 sample annealed at lower temperature ($<400°C$) contains hydroxyls and the samples are less crystalline (Fig. 1). But at $400°C$ the complete water content is lost and the recrystallisation starts. This is evident from the decrease in line width of XRD reflection by comparing the samples of powder B and C in Fig. 1. The evolved gas analyses shows that upto $400°C$ it is only H_2O as the product. Around $650°C$ pure phase of anatase is formed. Above this temperature mixed phases exists. But above $700°C$ the powders transform to rutile. The degussa P-25 sample was taken as such without any heat treatment for both XRD and photocatalysis, which had mixed phases of both anatase and rutile forms.

Kinetic data are shown in Fig. 2. The degradation process takes around 60 min for complete mineralisation of 128 ppm PAAB solution with powder C. From Fig. 2 it is evident that in the beginning the degradation process is slow but later it decreases quite rapidly. For the Degussa P-25 sample for complete mineralisation takes place around 6.5 h. It can also be observed that the process without any catalyst takes around 17 h, and with powder A around 15 h. Finally PAAB degradation is faster when TiO2 annealed at $650°C$ is used as the catalyst, which is of pure anatase form.

Referring to Table 1, the average crystallite size increases with the increasing temperature of annealing. From the table it is shown that the crystallite size of rutile form of TiO2 is higher. But the photocatalytic activity keeps increasing with temperature of annealing till TiO2 becomes pure anatase form. The crystallite size is high for rutile, but the catalytic activity is less compared to the anatase form. Crystallite size increases gradually with increase of temperature. As the size

increases there is decrease in surface area. This decrease in surface area should also show the decrease in efficiency [9,10]. The crystal structure and the surface area makes the anatase form more reactive. The difference in the lattice structure causes different mass densities and electronic band structures between the two forms of TiO2. (The Ti–Ti distances in anatase are greater where Ti–O distances are shorter than rutile. The TiO6 octahedron in anatase is significantly distorted compared to that of rutile.)

The differences in lattice structure cause the differences in electronic band structures between two forms of TiO2 [11]. As a result, the band gap increases and band edges shift to yield larger redox potentials. The solvent reorganisation free energy for charge transfer to a substrate however, remains unchanged. The increased driving force and the unchanged solvent reorganization free energy is making the anatase form of TiO2 a much better catalyst than the rutile form.

The degradation process was followed by the UV–visible spectrophotometry. The samples were withdrawn at several time intervals during the process of illumination. Five prominent peaks at 210, 263.6, 344.4, 387.2 and 405.9 nm were observed for the pure PAAB solution as shown in Fig. 3. The peaks at 210 and 263.6 nm should be because of the E_2-band and B-band of benzene ring present in the PAAB [12,13]. The azo group –N=N– is expected to absorb at 347 nm which is a $n \rightarrow \pi^*$ transition. The peak at 344.4 nm should be because of this –N=N– azo group. The λ_{max} for this compound is expected to be 387.8 nm. Which should be because of the chromophoric group present is the azo compound. The chromophoric group should be –N=N–, which is having two benzene rings on both the sides. This arrangement should be responsible for the absorption at 400 nm. After the illumination for 10 min, the small hump at 344 nm still persists. But the peak at 400 nm splits into a doublet which appears at 380 and 400 nm. When auxochromic group appear on the same ring as the chromophore both groups influence the absorption. The influence is most pronounced when an electron donating group and electron attracting group are *para* to one another. A covalently unsaturated group responsible for electron absorption is

Table 1
Details of material characteristics for various TiO2 samples

Sl. No.	TiO2 sample	Thermal treatment	Average crystal size is A^0 [a]	Phase content[b] A : R
1.	Degussa P-25	As received	147.591	70 : 30
2.	Powder A	120°C	50.616	100 : 00
3.	Powder B	400°C	159.511	100 : 00
4.	Powder C	650°C	177.528	100 : 00
5.	Powder D	700°C	222.62	00 : 100

[a]From Scherrer's equation relating the pure diffraction breadth (half band width) to crystallite size normal to the plane hkl as:

$$D_{hkl} = -\frac{K\lambda}{\beta \cos \Theta}$$

where D_{hkl} is the mean dimension in A^0, λ the wavelength, β the pure diffraction line broadening, Θ the Bragg angle of the reflection (hkl) and K is a constant approximately equal to unity. The half band width depends on crystallite size and microstrain in the lattice [7,8].
[b]Intensity ratio of (100) reflection to Anatase (A) and (110) of rutile (R) of XRD.
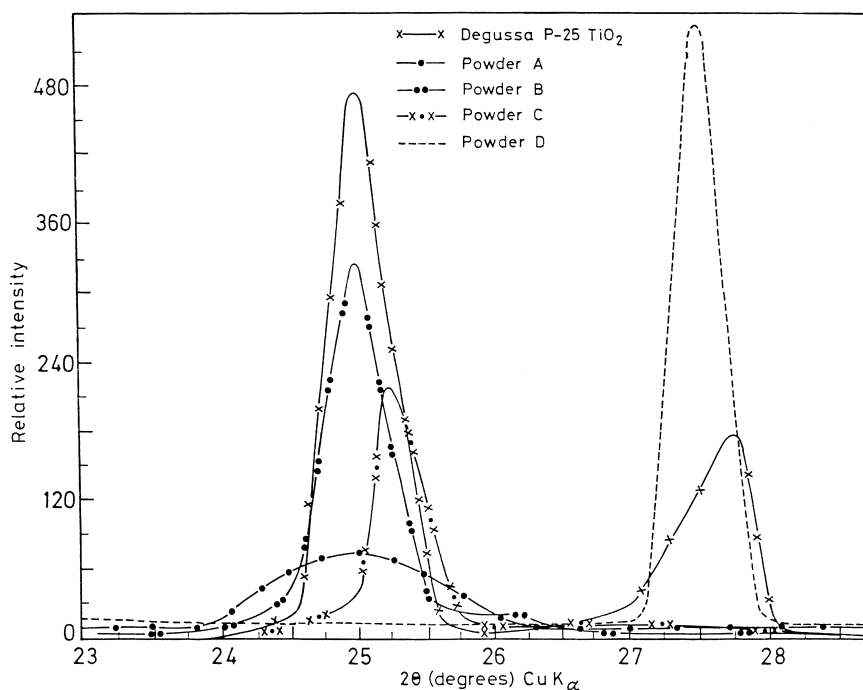
Fig. 1. XRD pattern of different TiO$_2$ samples showing the intensity ratio of (100) reflection of anatase (A) and (110) of rutile (R).

N=N or NO$_2$. The saturated group with nonbonded electron which when attached to a chromophore alters both the wavelength and the intensity of the absorption in the auxochromic group NH$_2$ with a lone pair of electrons. Because of this the compound formed should be nitro aniline. This should be only either o-nitro aniline or p-nitro aniline. If the compound is o-nitro aniline the peaks expected is 283 nm for $\pi \rightarrow \pi^*$ transition for the K-band and 412 nm for B-band. Both these peaks do appear in the spectra. Therefore one of the intermediate formed should be o-nitro aniline. If there is formation of p-nitro aniline then a peak at 381 nm for K-band and submerged peak for B-band is expected. A band is

observed at 380 nm. This should be because of p-nitro aniline. Therefore both o- and p-nitro aniline should have formed during the process of degradation. To check this a pure compound of p-nitro aniline is taken for the spectrum which is also shown is Fig. 3. Further, with illumination upto 60 min, the peak intensities decrease rapidly.

The UV–visible analysis for the PHAB is shown in Fig. 4. The original solution of PHAB shows peaks at 220 and 260 nm, and a broad peak at 300–400 nm whose maximum at 370 nm is observed. The peaks at 220 and 260 nm should be because of E$_2$-band and B-band of benzene. The peak at 370 nm should be the λ_{max} for this compound. This should
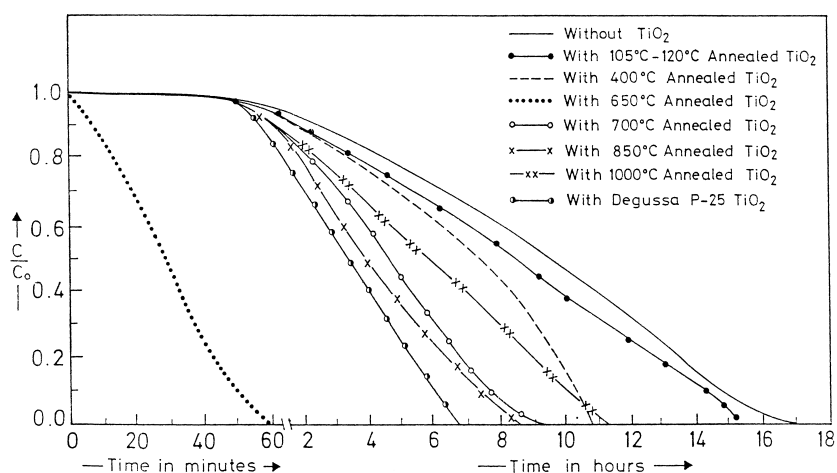

Fig. 2. Concentration versus time curves for photocatalyst TiO$_2$ annealed at different temperatures (from 105°C to 1000°C) and also for Degussa P-25 sample.
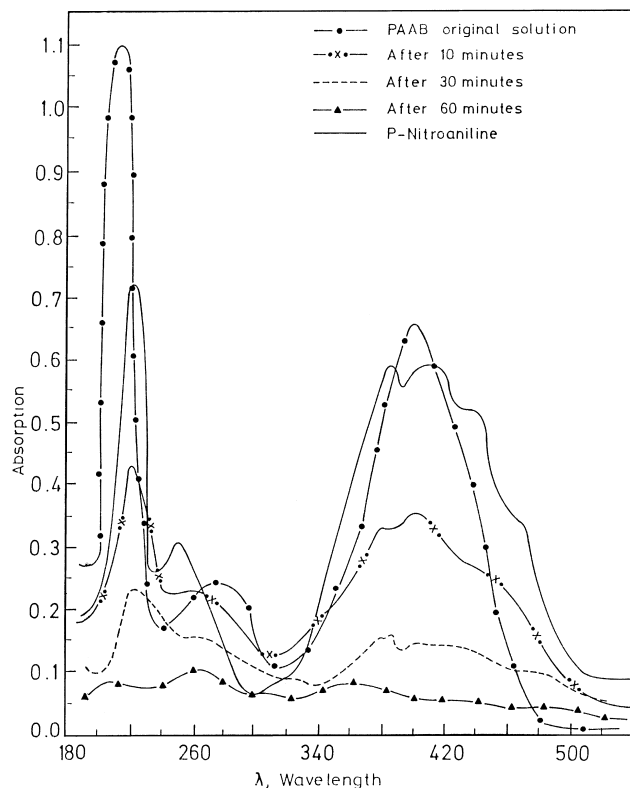
Fig. 3. UV–visible spectra of PAAB taken during the process of degradation using TiO$_2$ as the photocatalyst. (a) pure PAAB, (b) after 10 min, (c) after 30 min, (d) after 60 min, (e) pure *p*-nitro aniline.

be because of the two benzene rings and the –N=N– between them. The intermediates were analysed at the time intervals of 15 and 30 min. The 220 nm peak is shifted to 200 nm, a small peak at 280 nm has appeared. The peak of the original compound which appeared 370 nm has shifted very clearly
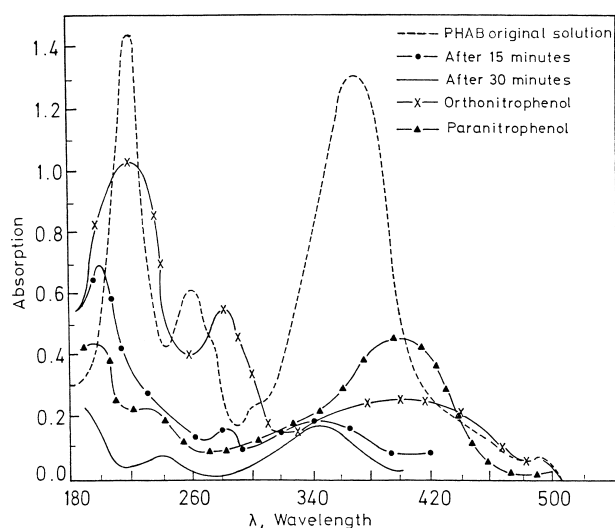

Fig. 4. UV–visible spectra of PHAB taken during the process of degradation using TiO$_2$ as the photocatalyst. (a) pure PHAB, (b) after 15 min, (c) after 30 min, (d) pure *o*-nitrophenol, (e) pure *p*-nitrophenol.

to 350 nm. The nitro phenol is expected to absorb at 279 and 351 nm. These two peaks may submerge with B-band of benzene and with azo group. *p*-nitrophenol is expected to absorb at 318 nm and the B-band is submerged. Because of submerging a very broad peak with two shoulders at 348.4 and 386.5 nm is observed. Therefore, *o*-nitrophenol and *p*-nitrophenol is formed during the process of degradation. The formation of *m*-nitrophenol also cannot be ruled out since all these bands appear at the same region and they are submerged.

Further in the IR study the spectra obtained is as shown in Fig. 5. The concentration of PAAB is increased to 0.825 mM so that this can be extracted into ethyl acetate. Spectra (a) is taken for the pure PAAB is in the solid state using KBr as the standard. The region A is due to the N–H stretching and the region B is for aromatic C–H stretching [12,13]. The region C is due to –N=N– stretching vibration of the azo group compound. *p*-substituted azo benzene should be responsible for the region D. The aromatic structure of the two benzene rings along with its substituents should be showing peaks in the region E. The other spectra shown in Fig. 5 are taken during several time intervals, during the process of degradation which was further extracted into ethyl acetate. Subtraction results of PAAB with ethyl acetate is presented in Fig. 5. Due to certain structural characteristics the region A in these spectra becomes very broad. During the process of degradation
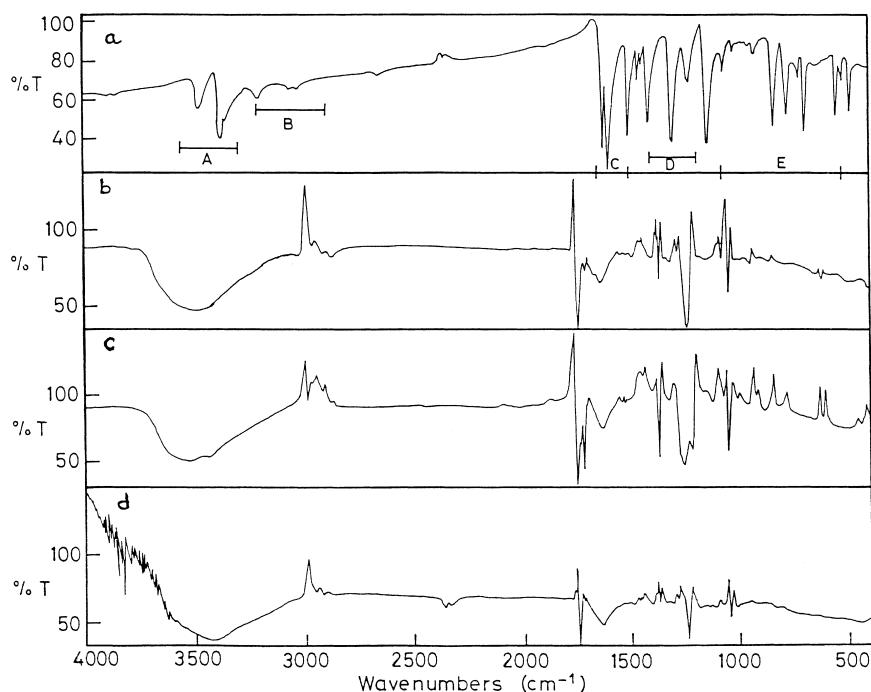
Fig. 5. IR spectrum of (a) pure PAAB solid spectra, (b) subtraction result of PAAB with ethyl acetate after 1 h, (c) subtraction result of PAAB with ethyl acetate after 2.5 h, (d) subtraction result of PAAB with ethyl acetate after 5 h.

the aromatic C–H stretching increases in intensity as shown in spectra (c) but later even this decreases. The region C which is due to –N=N– stretching vibration has clearly shifted from 1630 to 1745 cm^{-1}. This should be because of the NO_2 group formation which is bonded to the benzene ring whose intensity also decreases rapidly with the time.

4. Conclusion

Anatase form (TiO_2 annealed at 600–650°C) can efficiently photocatalyse the degradation process of PAAB and PHAB compared to the rutile form (annealed above 700°C) and also to Degussa P-25 sample. The intermediates recognised by UV–visible spectroscopy during the process of degradation for PAAB is *o-* and *p*-nitro aniline. For the PHAB it is the *o-* and *p*-nitro phenol.

References

[1] H. Zollinger, Color Chemistry – Synthesis properties and application of organic dyes and pigments, VCH, New York, 1981, p. 92.
[2] Jack T. Spadaro, Lorne Isabelle, V. Ranganathan, Environ. Sci. Technol. 28 (1994) 1389.
[3] M. Audaithai, T.R.N. Kutty, Mater. Res. Bull. 22 (1987) 641.
[4] Hatchard, Parker, Proc. Soc. Ser., A 235 (1956) 518.
[5] Hatchard, Parker, Proc. Roy. Soc. Ser., 220 (1953) 104.
[6] J. Lee, H.H. Seliger, J. Chem. Phys. 40 (1964) 519.
[7] Anthony R. West, Solid State Chemistry and its Application, Wiley, 1984.
[8] B.E. Warren, X-ray Diffraction, Addison Wesley, 1969.
[9] Hisashi Harada, Toyotoshi Ueda, Chem. Phys. Lett. 106(3) (1984) 229.
[10] T. Sakta, T. Kawai, K. Hashimoto, Chem. Phys. Lett. 50 (1982) 88.
[11] Amy L. Linsebigler, Guangguan Lu, John T. Yates Jr., , Chem. Rev. 95 (1995) 735.
[12] Silverstein, Bassler, Morril, Spectroscopic Identification of Organic Compounds, 4th ed., Wiley, 1981.
[13] John. R. Dyer, Applications of Absorption Spectroscopy of Organic Compounds, Prentice Hall, Englewood Cliffs.